Nature of the chemical bonding in D_{3h} [MH₃M]⁺ cations (M = Be, Mg)

Fabio E. Penotti,[1] David L. Cooper,[2] Peter B. Karadakov,[3] and Robert Ponec[4]

[1] *F. E. Penotti*
Consiglio Nazionale delle Ricerche, Istituto di Scienze e Tecnologie Chimiche "Giulio Natta", Via Golgi 19, I-20133 Milano MI, Italy
[2] *D. L. Cooper*
Department of Chemistry, University of Liverpool, Liverpool L69 7ZD, United Kingdom
[3] *P. B. Karadakov*
Department of Chemistry, University of York, Heslington, York YO10 5DD, United Kingdom
[4] *R. Ponec*
Institute of Chemical Process Fundamentals, Czech Academy of Sciences Prague 6, Suchdol 2, 165 02 Czech Republic

ABSTRACT

Motivated by the particularly short metal-metal distance that has been predicted for the D_{3h} [BeH₃Be]⁺ cation, comparable to those anticipated for triple bonds, we investigate the nature of the bonding interactions in the D_{3h} [MH₃M]⁺ cations (M = Be, Mg). CCSD(T)/cc-pVQZ calculations are used to determine optimized geometries for all of the various species, including those 'capped' by He or Ne atoms (as proxies for an inert gas matrix). The primary tools that are then used to investigate the nature of the chemical bonding are spin-coupled generalized valence bond calculations and the analysis of localized natural orbitals and of domain-averaged Fermi holes. The various results for all of the systems considered indicate the presence of highly polar three-center two-electron M−H−M bonding character instead of any significant direct metal-metal bonding.

Introduction

In spite of the obvious deterrence for experimentalists of the high toxicity of beryllium compounds,[1] a great deal is now known about the organometallic and coordination chemistry of beryllium.[2] Beryllium compounds that have been studied experimentally and especially computationally include various systems that feature BeBe bonding and/or very short BeBe distances.[3-19] For example, it has been shown for various choices of X, such as a fluorine atom or an appropriate N-heterocyclic carbene ligand, that certain XBeBeX species feature Be–Be bonds that are both significantly stronger and shorter than the weak and rather long bond in Be₂.[3-4] We note that Liu et al. have interpreted the bonding in the octahedral Be₂(μ₂-Li)₄ cluster, and others, in terms of a Be=Be double-π bond[10] and the bonding in Be₂X₄Y₂ clusters (X = Li, Na

and Y = Li, Na, K) in terms of Be≡Be triple bonds.[15] Calculations and analysis carried out by Rohman et al. also support the notion of Be≡Be triple bonds in various systems, including Be₂X₆ (X = Li, Na), but they found the BeBe bonding to be ultra-weak in spite of the very short BeBe distances.[16-17] Indeed, some systems have been studied both experimentally and computationally, such as the rhombic Be₂O₂ cluster, which feature very short BeBe distances in the absence of any direct BeBe chemical bonding.[8-9, 11]

There has been significant recent computational interest in predicting the existence of potentially stable beryllium complexes that feature ultra-short BeBe distances,[6, 12-13, 18-19] regardless of whether or not they actually involve any direct chemical bonds between the beryllium atoms. The present work was motivated by one such study in which three bridging hydrogen atoms

were used potentially to simulate the effect of a Be≡Be triple bond, with the outcome that particularly short BeBe distances were predicted for various systems, including the D_{3h} [BeH₃Be]⁺ cation.[13] Our main goal here is to investigate the nature of the bonding interactions in this type of system, especially the D_{3h} [MH₃M]⁺ cations (M = Be, Mg), including those 'capped' by He or Ne atoms (as proxies for an inert gas matrix). To this end, we follow all-electron CCSD(T)/cc-pVQZ geometry optimizations with spin-coupled generalized valence bond (SCGVB) calculations and the analysis of localized natural orbitals and domain-averaged Fermi holes.

It is our expectation that the various systems we study should all correspond to local minima on their respective potential energy surfaces and that their electronic structures are somewhat more likely to involve highly polar three-center two-electron (3c-2e) M–H–M bonding character rather than direct metal-metal chemical bonds. We note in this context that Kalita et al.[14] detected in the LiMH₂MLi system (M =Be, Mg, Ca) with two bridging H atoms the presence of two 3c-2e M–H–M bonds that were said to be reminiscent of the bonding situation in diborane. As is well known, the introduction of the 3c-2e bonding motif[20] for electron deficient systems led to great advances in the understanding of many classes of molecules, including boron hydrides.[21-22]

Theoretical and computational details

The geometries of various D_{3h} [MH₃M]⁺ cations (M = Be, Mg), including those 'capped' by noble gas (Ng) atoms He or Ne (as represented in Figure 1), were optimized at the all-electron CCSD(T)/cc-pVQZ level using MOLPRO.[23-24] We then checked in each case that all of the vibrational frequencies were positive, thereby confirming that we have located local minima. All of the subsequent calculations and analysis were carried out at these optimized geometries, using cc-pVQZ basis sets throughout.
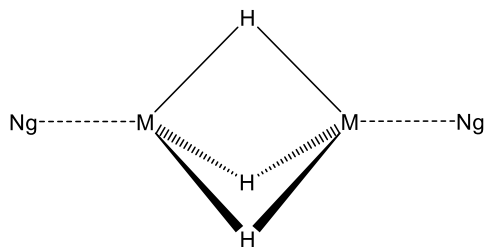

Figure 1. Schematic representation of the geometries of D_{3h} [NgMH₃MNg]⁺ cations.

The spin-coupled generalized valence bond (SCGVB) wavefunctions considered here for the six valence electrons of the MH₃M moieties take the form

$$\Psi_{\text{SCGVB}(6)}$$
$$= \mathcal{A}\left\{(\text{closed-shell orbitals})\left(\prod_{i=1}^{6}\phi_i\right)\Theta_{0,0}^{6}\right\}$$

(1)

in which the ϕ_i are the six singly-occupied nonorthogonal active orbitals and the total active space spin function $\Theta_{0,0}^{6}$ is a linear combination of all five linearly independent ways that the spins of these six electrons can be coupled to yield a state with $S = 0$ and $M_S = 0$.[25] All of the closed-shell and active orbitals were fully optimized as expansions in the full molecular basis set, simultaneously with the expansion coefficients of $\Theta_{0,0}^{6}$. All of these SCGVB(6) calculations were carried out using the CASVB module[26-30] in MOLPRO.[23-24]

We also calculated the corresponding '6 electron in 6 orbitals' complete active space self-consistent field, i.e. CASSCF(6,6), wavefunctions. Additionally, full-valence CASSCF calculations, with all allowed distributions of six electrons in eleven orbitals, were carried out for the 'bare' D_{3h} [MH₃M]⁺ cations (M = Be, Mg); such CASSCF(6,11) calculations were also carried out for the corresponding systems capped by Ng (Ng = He, Ne) atoms. All of these various CASSCF wavefunctions were generated using MOLPRO.[23-24]

In addition to examining the highly-visual SCGVB(6) descriptions of these various systems, we also performed domain-averaged Fermi hole (DAFH) analysis.[31-37] It proved especially informative to consider 'holes' that are averaged over multi-atom domains, each formed as the union of individual quantum theory of atoms in molecules (QTAIM) domains.[38] Such DAFH analysis not only provides information about any electron pairs that remain intact within each of the chosen fragments but also about the broken or dangling valences that are created by the (formal) bond splitting that would be required to isolate that fragment from the rest of the molecule. With this in mind, we took one domain to be the union of the two M atom QTAIM domains and another to be the complementary domain formed from the union of the three H atom QTAIM domains. In this way, we can detect whether there is any direct MM bonding and we can identify the nature of the MHM interactions.

In the special case that the domain is taken instead to be the whole molecule, i.e. exhausting the complete space, DAFH analysis corresponds to the generation of localized natural orbitals (LNOs). All of the DAFH and LNO analysis described in the present work used our own codes, with the required QTAIM analysis[38] carried out with AIMAll.[39] Using the same isovalue throughout, pictorial depictions of SCGVB orbitals, LNOs and DAFH functions were produced using Virtual Reality Markup Language (VRML) files generated with Molden.[40]

Results and discussion

Key geometrical parameters for D_{3h} [MH$_3$M]$^+$ and [NgMH$_3$MNg]$^+$ cations, optimized at the all-electron CCSD(T)/cc-pVQZ level of theory, are presented in Table 1. Our values for the beryllium species are very similar to those reported by Zhao et al.,[13] with the small differences being mostly due to the use here of a different basis set. Whether M is Be or Mg, we observe from Table 1 that the capping of D_{3h} [MH$_3$M]$^+$ cations with Ng atoms leads only to very small increases in the MHM angle and thus

in the MM distances, but it has practically no effect on the MH distances. The observation of such small changes to the D_{3h} geometries indicates that there are only relatively weak interactions with the Ng atoms. As such we can anticipate that the nature of the bonding interactions in the central MH$_3$M moieties should change relatively little when the D_{3h} [MH$_3$M]$^+$ cations are capped with He or Ne atoms.

Table 1. Distances (Å) and angles (degrees) for D_{3h} [MH$_3$M]$^+$ and [NgMH$_3$MNg]$^+$ cations, optimized at the all-electron CCSD(T)/cc-pVQZ level of theory.

M	Ng	r_{MM}	r_{MH}	r_{NgM}	θ_{MHM}
Be		1.672	1.451		70.37
Be	He	1.676	1.450	1.475	70.64
Be	Ne	1.679	1.451	1.702	70.71
Mg		2.330	1.839		78.63
Mg	He	2.336	1.839	1.969	78.85

Our BeBe distances turn out to be very slightly smaller (by about 0.01 Å) than the already small values found by Zhao et al..[13] We notice that the BeBe separations in the D_{3h} [NgBeH$_3$BeNg]$^+$ cations are ca. 0.04 Å shorter than those found for the rhombic Be$_2$O$_2$ cluster.[8-9, 11] We are not aware of any previously reported geometries for the magnesium systems. We find that the MgMg separation in the D_{3h} [HeMgH$_3$MgHe]$^+$ cation is shorter by ca. 0.03 Å than was found for the rhombic Mg$_2$O$_2$ cluster.[9, 11]

The total energies from calculations at various levels of theory are reported in Table S1 in the Supporting Information. For each system, the energy difference between the SCGVB(6) and the corresponding CASSCF(6,6) descriptions was very small (ca. 3 kJ/mol); the SCGVB(6) wavefunctions for the various Be and Mg systems incorporate more than 96.8% and 99.4%, respectively, of the non-dynamical correlation energy that is retrieved with the CASSCF(6,6) calculations. Increasing the number of active orbitals to 11, as in CASSCF(6,11), retrieved further energy lowerings in each case of ca. 120 kJ/mol. Much larger energy improvements are of course associated with the

dynamical correlation incorporated in the all-electron CCSD(T) calculations. It remains to be seen, however, whether our various modes of analysis reveal any significant differences in the nature of the bonding when we switch to different levels of theory.

Beryllium systems

We start by considering the nature of the SCGVB(6) descriptions of the bonding in the D_{3h} $[MH_3M]^+$ cation. Although these calculations were carried out without imposing any symmetry relations amongst the active orbitals, we found in each case that the converged solution features two sets of three symmetry-related orbitals, with each 'pair' being primarily associated with a particular Be–H–Be linkage. Symmetry-unique active orbitals ϕ_1 and ϕ_2 for D_{3h} $[BeH_3Be]^+$ are depicted as the first two images in the top row of Figure 2. The remaining active orbitals for this cation are related to these two by successive $\hat{C}_3$ rotations around the principal axis. Whereas SCGVB orbital ϕ_1 has distinct three-center BeHBe character, orbital ϕ_2 is somewhat more localized on the H atom. The orbital overlap $\langle\phi_1|\phi_2\rangle$ is 0.846 and we find that the perfect-pairing mode of spin coupling dominates the total active space spin function $\Theta_{0,0}^6$, with a weight of 98.3% in the Kotani basis, so that the spins associated with ϕ_1 and ϕ_2 are predominantly coupled to a singlet. The observation that both of ϕ_1 and ϕ_2 have high amplitudes on the bridging H atom suggests that there is high polarity in the BeHBe units. All of this means that the SCGVB(6) description of the D_{3h} $[BeH_3Be]^+$ cation corresponds primarily to three equivalent highly polar three-center two-electron (3c-2e) M–H–M bonding units, each reminiscent of those in diborane.

As can be seen from Figures S2 and S3 in the Supporting Information, the corresponding SCGVB(6) orbitals for the D_{3h} $[NgBeH_3BeNg]^+$ cations (Ng = He, Ne) are rather difficult to distinguish by eye from those for the 'bare' system; taken together with the dominance of

the perfect-pairing mode of spin coupling, the SCGVB(6) descriptions for each of the 'capped' systems again corresponds primarily to three equivalent highly polar 3c-2e Be–H–Be bonding units.
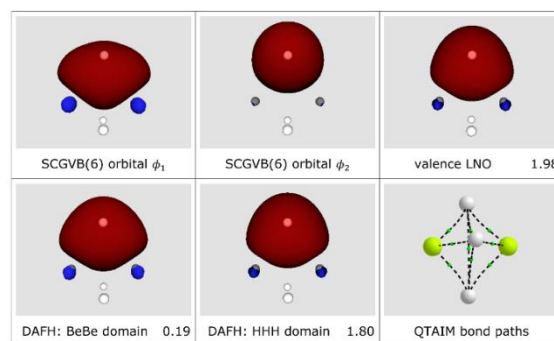

Figure 2. Symmetry-unique key valence functions (and occupation numbers where appropriate) from analysis of the SCGVB(6) description of the D_{3h} $[BeH_3Be]^+$ cation. Also shown are QTAIM bond paths.

We turn now to outcomes of DAFH analysis for the D_{3h} $[BeH_3Be]^+$ SCGVB(6) wavefunction. In addition to the one-electron density and QTAIM analysis as input, full DAFH analysis for non-exhaustive (combinations of) individual QTAIM domains requires in this case the use of the two-electron density, which was readily available to us in the case of SCGVB and CASSCF wavefunctions. Such DAFH analysis for the domain comprising the union of the two beryllium atom QTAIM domains produces three symmetry-equivalent valence functions, each populated by 0.19 electrons (see the first image in the second row of Figure 2). Such an occupation number of 0.19 can be understood as the joint contribution from the two metal atoms to a shared electron pair of a particular 3c-2e Be–H–Be linkage. The corresponding DAFH analysis for the domain consisting of the union of the three hydrogen atom QTAIM domains also produces three symmetry-equivalent valence functions (see the second image in the second row of Figure 2). Each of these functions has an occupation number of 1.80, which can be understood as the complementary contribution

to the shared electron pair of a particular 3c-2e Be−H−Be linkage. The considerable disparity between the occupation numbers from complementary BeBe and HHH domains (0.19 and 1.80, respectively) indicates that the electron pair in each Be−H−Be linkage is shared very unevenly, with high polarity across the three centers. The occupation numbers of the other non-core functions produced by the DAFH analysis were all sufficiently small that we did not examine them in any detail.

The existence of the three 3c-2e Be−H−Be bonding units is also straightforwardly corroborated by the forms of the localized natural orbitals (LNOs) that result from simpler DAFH analysis performed for the domain involving the whole molecule. Such analysis still requires the one-electron density and QTAIM analysis as input, but not the two-electron density. We find that it yields in this case three degenerate valence LNOs with occupancies close to two. The forms of these LNOs (see the third image in the top row of Figure 2) are again strongly suggestive of three equivalent highly polar 3c-2e Be−H−Be bonding units. The occupation numbers of all of the remaining non-core LNOs were sufficiently small that we did not examine them in any detail.

As can be seen from Figures S2 and S3 in the Supporting Information, there were no significant differences in the corresponding valence LNOs and DAFH functions for the D_{3h} [NgBeH$_3$BeNg]$^+$ SCGVB(6) wavefunctions. At most we observed fairly small changes in occupation numbers, on the order of 0.01. We have also examined the corresponding valence LNOs and DAFH functions for D_{3h} [BeH$_3$Be]$^+$ and [NgBeH$_3$BeNg]$^+$ cations using different levels of theory, including CASSCF(6,11), CCSD and B3LYP. We found that there were slightly larger (but still very small) changes to occupation numbers but negligible changes to the forms of the various functions. (Note that for the DAFH analysis for BeBe and HHH domains at the CCSD and B3LYP levels of theory we used a reliable one-electron approximation[35] based on natural orbital occupation numbers.[41]) As a representative demonstration of the high similarity between these different sets of analyses we display in Figures S4 and S5 in the Supporting Information the dominant symmetry-unique valence LNOs that were obtained at different levels of theory.

We now examine the QTAIM bond paths for the D_{3h} [BeH$_3$Be]$^+$ cation, calculated using the SCGVB(6) wavefunction. These are depicted in the third image in the second row of Figure 2. (Note that in addition to the bond critical points, which are shown, there are corresponding ring and cage critical points, which have not been displayed.) Clearly there are curved bond paths linking Be and H atoms. There are also corresponding bond paths linking the H atoms, but no BeBe bond path. Indeed, the critical point at the center of this cation turns out to be a ring critical point, sandwiched between two cage critical points along the BeBe axis. We checked that the pattern of critical points and of bond paths was unchanged when we switched from SCGVB(6) to CASSCF(6,11), CCSD or B3LYP descriptions. (Additionally, as can be seen from the third image in the second row of Figure S2 in the Supporting Information, the basic pattern in the BeH$_3$Be moiety was unchanged upon capping the 'bare' cation with He atoms.)

Additional corroboration for the absence of any significant direct bonding between the beryllium centers is provided by various indicators of the metal-metal bond order, for which we report here the values of two somewhat different quantities. The first of these is the shared-electron distribution index (SEDI),[42] also known as a delocalization index,[43] which provides a measure of the distribution of the electrons that are shared between two atomic domains. The other, denoted here as W_{AB}, is based on an improved definition of two-center Wiberg-Mayer bond orders for correlated singlet systems,[44] but re-expressed in AIM-generalized form.[11, 45] The values of SEDI(Be,Be) and of W_{BeBe} for the SCGVB(6) description of the D_{3h} [BeH$_3$Be]$^+$ cation turn out to be just 0.033 and 0.027, respectively, providing further confirmation of

the absence of any significant direct metal-metal bonding. (Analogous small values were found for the D_{3h} [NgMH$_3$MNg]$^+$ cations and we checked that changing the level of theory to CASSCF(6,11), CCSD or B3LYP, using the same cc-pVQZ basis sets, did not lead to significant changes.)

Clearly there is no evidence in the forms of any of the valence LNOs, DAFH functions or SCGVB orbitals, or in bond indices and QTAIM analysis, for any significant direct BeBe bonding in the D_{3h} [BeH$_3$Be]$^+$ and [NgBeH$_3$BeNg]$^+$ cations (Ng = He, Ne) at their all-electron CCSD(T)/cc-pVQZ geometries. Instead the two positively-charged beryllium centers are held together with a very short BeBe distance by the three negatively-charged hydrogen centers, with a stabilizing contribution from three equivalent sets of highly polar 3c-2e Be–H–Be bonding character.

Magnesium systems

We carried out essentially the same modes of analysis for the D_{3h} [MgH$_3$Mg]$^+$ and [HeMgH$_3$MgHe]$^+$ cations as we have described for the beryllium systems. Again we found, without the imposition of any symmetry relations amongst the active orbitals, that the converged SCGVB(6) solutions for the 'bare' D_{3h} [MgH$_3$Mg]$^+$ cation features two sets of three symmetry-related orbitals, with each 'pair' being primarily associated with a particular Mg–H–Mg linkage (see first two images in the top row of Figure 3). The orbital overlap $\langle \phi_1 | \phi_2 \rangle$ is 0.825 and the total active space spin function, $\Theta_{0,0}^6$, is again dominated by the perfect-pairing mode: this system features three symmetry-equivalent highly polar 3c-2e Mg–H–Mg bonding units, albeit SCGVB orbital ϕ_1 appears to have a larger relative contribution from H than was the case for the various beryllium species. The dominant valence LNOs for the D_{3h} [MgH$_3$Mg]$^+$ cation consist of three almost doubly-occupied symmetry-equivalent orbitals that are consistent with notions of 3c-2e character (see the third

image in the top row of Figure 3). Except again for a larger relative contribution from H, there are obvious similarities to the bonding situation that we found for the beryllium species.
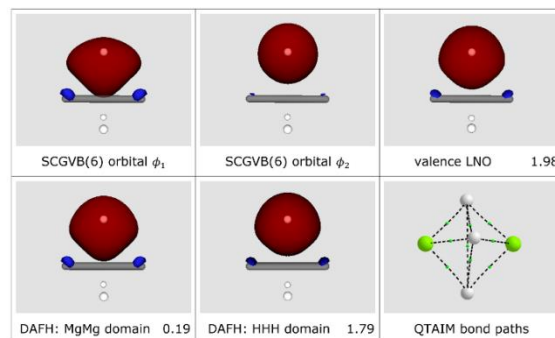

Figure 3. Symmetry-unique key valence functions (and occupation numbers where appropriate) from analysis of the SCGVB(6) description of the D_{3h} [MgH$_3$Mg]$^+$ cation. Also shown are QTAIM bond paths.

Much the same turns out to be true for the dominant valence functions generated by means of DAFH analysis for the MgMg and HHH domains (see the first two images in the second row of Figure 3). Even the two occupation numbers of 0.19 and 1.79, representing the relative contributions to each Mg–H–Mg bonding unit from the MgMg and HHH domains, respectively, are much the same as in the beryllium systems. Unsurprisingly, the corresponding valence LNOs, DAFH functions and SCGVB orbitals for the D_{3h} [HeMgH$_3$MgHe]$^+$ cation (see Figure S7 in the Supporting Information) turn out to be difficult to distinguish by eye from those for [MgH$_3$Mg]$^+$. Similarly, except for small changes in occupation numbers, we found that changing the level of theory had negligible effects on the valence LNOs and DAFH functions (see Figures S8 and S9 in the Supporting Information for depictions of the various LNOs).

The QTAIM bond paths for the D_{3h} [MgH$_3$Mg]$^+$ cation are depicted in the third image in the second row of Figure 3. (As before, the ring and cage critical points have not been displayed.) The

pattern is the same as we saw for the D_{3h} [BeH$_3$Be]$^+$ cation, confirming the similarity between these two systems: there are curved bond paths linking Mg and H atoms, as well as linking H atoms, but there is no MgMg bond path. As can be seen from the third image in the second row of Figure S7 in the Supporting Information, the basic pattern in the central moiety is unchanged upon capping the 'bare' D_{3h} [MgH$_3$Mg]$^+$ cation with He atoms. The values of SEDI(Mg,Mg) and of W_{MgMg} for the D_{3h} [MgH$_3$Mg]$^+$ cation turn out to be just 0.039 and 0.033, respectively, providing further confirmation of the absence of any significant direct metal-metal bonding.

As was the case for the corresponding beryllium systems, there is no evidence in the forms of any of the valence LNOs, DAFH functions or SCGVB orbitals, or in bond indices and QTAIM analysis, for any significant direct MgMg bonding in the D_{3h} [MgH$_3$Mg]$^+$ and [HeMgH$_3$MgHe]$^+$ cations at their all-electron CCSD(T)/cc-pVQZ geometries. As before, we conclude that the two positively-charged metal centers are held together with a short MM distance by the three negatively-charged H centers, with a stabilizing contribution from three equivalent sets of highly polar 3c-2e M−H−M bonding character.

We also briefly examined the 'mixed' system, *i.e.* the C_{3v} [BeH$_3$Mg]$^+$ cation, for which geometrical parameters and total energies are presented in Tables S2 and S3 in the Supporting Information, respectively. As might have been expected, the resulting valence LNOs, DAFH functions and SCGVB orbitals (see Figures S10 to S13 in the Supporting Information) turn out to be 'mixed', closely resembling those for the D_{3h} [BeH$_3$Be]$^+$ cation on the beryllium side of the 3c-2e Be−H−Mg bonding units and resembling those for the D_{3h} [MgH$_3$Mg]$^+$ cation on the magnesium side.

We observe that the BeMg separation in the D_{3h} [BeH$_3$Mg]$^+$ cation is shorter by *ca.* 0.04 Å than was found for the BeMgO$_2$ ring[11] but, consistent with the situation in the D_{3h} [BeH$_3$Be]$^+$ and [MgH$_3$Mg]$^+$ cations, we find that there is no

BeMg QTAIM bond path (see Figures S10 and S11 in the Supporting Information, but one small difference is that there are also no longer any bond paths linking the H atoms in the 'mixed' case). The values of SEDI(Be,Mg) and of W_{BeMg} of just 0.031 and 0.027, respectively, provide further confirmation of the absence of any significant direct metal-metal bonding in the C_{3v} [BeH$_3$Mg]$^+$ cation, in spite of the short BeMg separation.

Conclusions

The present work was motivated by a recent study that reported particularly short BeBe separations for various cations based on a central D_{3h} BeH$_3$Be moiety,[13] with the presence of the three bridging hydrogen atoms being claimed to simulate the effect of a Be≡Be triple bond.[13] We have carried out all-electron CCSD(T)/cc-pVQZ geometry optimization for the D_{3h} [MH$_3$M]$^+$ cations (M = Be, Mg), with and without 'capping' by He or Ne atoms (as proxies for an inert gas matrix). In order to investigate the nature of the chemical bonding we then used SCGVB and CASSCF calculations (amongst others), together with the analysis of valence localized natural orbitals and domain-averaged Fermi holes, as well as bond indices and QTAIM bond paths. We also briefly examined the 'mixed' system, *i.e.* the C_{3v} [BeH$_3$Mg]$^+$ cation.

In each case we found no evidence for any significant direct metal-metal bonding. Instead the short separations are the result of the positively-charged metal centers being held close together by the three negatively-charged hydrogen centers, with a stabilizing contribution from three equivalent sets of highly polar 3c-2e M−H−M bonding character.

We concur with Zhao et al.[13] that the D_{3h} [BeH$_3$Be]$^+$ cation is a very interesting target for experimental work, whether it involves trapping the 'bare' cations in inert gas matrices or potentially isolating species based on [L→MH$_3$M'←L]$^+$ moieties. The present work shows that the same turns out to be true for the

D_{3h} [MgH$_3$Mg]$^+$ cation and even for the 'mixed' C_{3v} [BeH$_3$Mg]$^+$ cation.

Keywords: Ultra-short metal-metal distances; Spin-coupled generalized valence bond (SCGVB) calculations; Localized natural orbitals; Domain-averaged Fermi hole analysis; Three-center two-electron bonding.

Additional Supporting Information may be found in the online version of this article.

References and Notes

[1]   World Health Organization, *Concise International Chemical Assessment Document 32: Beryllium and Beryllium Compounds*, WHO, Geneva, **2001**.

[2]   K. J. Iversen, S. A. Couchman, D. J. D. Wilson, J. L. Dutton, *Coord. Chem. Rev.* **2015**, *297-298*, 40-48.

[3]   S. A. Couchman, N. Holzmann, G. Frenking, D. J. D. Wilson, J. L. Dutton, *Dalton Trans.* **2013**, *42*, 11375-11384.

[4]   Z.-h. Cui, W.-s. Yang, L. Zhao, Y.-h. Ding, G. Frenking, *Angew. Chem. Int. Ed.* **2016**, *55*, 7841-7846.

[5]   K. Nijesh, S. De, P. Parameswaran, *Dalton Trans.* **2016**, *45*, 7836-7846.

[6]   C. Yuan, X.-F. Zhao, Y.-B. Wu, X. Wang, *Angew. Chem. Int. Ed.* **2016**, *55*, 15651-15655.

[7]   X.-F. Zhao, H. Li, C.-X. Yuan, Y.-Q. Li, Y.-B. Wu, Z.-X. Wang, *J. Comput. Chem.* **2016**, *37*, 261-269.

[8]   Q. Zhang, W.-L. Li, L. Zhao, M. Chen, M. Zhou, J. Li, G. Frenking, *Chem. Eur. J.* **2017**, *23*, 2035-2039.

[9]   W.-L. Li, J.-B. Lu, L. Zhao, R. Ponec, D. L. Cooper, J. Li, G. Frenking, *J. Phys. Chem. A* **2018**, *122*, 2816-2822.

[10]   X. Liu, M. Zhang, S. Yu, Y. Geng, X. Zhang, Y. Ding, Z. Su, *PCCP* **2018**, *20*, 23898-23902.

[11]   R. Ponec, D. L. Cooper, *J. Mol. Model.* **2018**, *24*, 226.

[12]   Z.-Z. Qin, Q. Wang, C. Yuan, Y.-T. Yang, X.-F. Zhao, D. Li, P. Liu, Y.-B. Wu, *Dalton Trans.* **2018**, *47*, 4707-4713.

[13]   X.-F. Zhao, C. Yuan, S.-D. Li, Y.-B. Wu, X. Wang, *Dalton Trans.* **2018**, *47*, 14462-14467.

[14]   A. J. Kalita, S. S. Rohman, C. Kashyap, S. S. Ullah, S. Reza, B. Borah, A. K. Guha, *Comput. Theor. Chem.* **2019**, *1167*, 112606.

[15]   X. Liu, R. Zhong, M. Zhang, S. Wu, Y. Geng, Z. Su, *Dalton Trans.* **2019**, *48*, 14590-14594.

[16]   S. S. Rohman, C. Kashyap, S. S. Ullah, A. K. Guha, L. J. Mazumder, P. K. Sharma, *ChemPhysChem* **2019**, *20*, 516-518.

[17]   S. S. Rohman, C. Kashyap, S. S. Ullah, L. J. Mazumder, P. P. Sahu, A. Kalita, S. Reza, P. P. Hazarika, B. Borah, A. K. Guha, *Chem. Phys. Lett.* **2019**, *730*, 411-415.

[18]   W.-Y. Tong, T.-T. Zhao, X.-F. Zhao, X. Wang, Y.-B. Wu, C. Yuan, *Dalton Trans.* **2019**, *48*, 15802-15809.

[19]   T.-T. Zhao, X.-F. Zhao, J.-H. Bian, W.-Y. Tong, B. Jin, X. Wang, C. Yuan, Y.-B. Wu, *Dalton Trans.* **2019**, *48*, 6581-6587.

[20]   H. G. Longuet-Higgins, *J. Chim. Phys.* **1949**, *46*, 268-275.

[21]   W. N. Lipscomb, *Acc. Chem. Res.* **1973**, *6*, 257-262.

[22]   W. N. Lipscomb, *Science* **1977**, *196*, 1047.

[23]   H.-J. Werner, P. J. Knowles, G. Knizia, F. R. Manby, M. Schütz, P. Celani, W. Györffy, D. Kats, T. Korona, R. Lindh, A. Mitrushenkov, G. Rauhut, K. R. Shamasundar, T. B. Adler, R. D. Amos, S. J. Bennie, A. Bernhardsson, A. Berning, D. L. Cooper, M. J. O. Deegan, A. J. Dobbyn, F. Eckert, E. Goll, C. Hampel, A. Hesselmann, G. Hetzer, T. Hrenar, G. Jansen, C. Köppl, S. R. Lee, Y. Liu, A. W. Lloyd, Q. Ma, R. A. Mata, A. J. May, S. J. McNicholas, W. Meyer, T. F. Miller III, M. E. Mura, A. Nicklass, D. P. O'Neill, P. Palmieri, D. Peng, K. Pflüger, R. Pitzer,

M. Reiher, T. Shiozaki, H. Stoll, A. J. Stone, R. Tarroni, T. Thorsteinsson, M. Wang, M. Welborn, *MOLPRO, version 2019.2, a package of ab initio programs*, Cardiff, U. K., see www.molpro.net.

[24] H.-J. Werner, P. J. Knowles, G. Knizia, F. R. Manby, M. Schütz, *WIREs Comput. Mol. Sci.* **2012**, *2*, 242-253.

[25] R. Pauncz, *The Symmetric Group in Quantum Chemistry*, CRC Press, Boca Raton, **1995**.

[26] T. Thorsteinsson, D. L. Cooper, J. Gerratt, P. B. Karadakov, M. Raimondi, *Theor. Chim. Acta* **1996**, *93*, 343-366.

[27] T. Thorsteinsson, D. L. Cooper, *Theor. Chim. Acta* **1996**, *94*, 233-245.

[28] D. L. Cooper, T. Thorsteinsson, J. Gerratt, *Int. J. Quantum Chem.* **1997**, *65*, 439-451.

[29] D. L. Cooper, T. Thorsteinsson, J. Gerratt, *Adv. Quantum Chem.* **1999**, *32*, 51-67.

[30] T. Thorsteinsson, D. L. Cooper, in *Quantum Systems in Chemistry and Physics, Vol 1: Basic Problems and Model Systems* (Eds.: A. Hernández-Laguna, J. Maruani, R. McWeeny, S. Wilson), Kluwer, Dordrecht, **2000**.

[31] R. Ponec, *J. Math. Chem.* **1997**, *21*, 323-333.

[32] R. Ponec, A. J. Duben, *J. Comput. Chem.* **1999**, *20*, 760-771.

[33] R. Ponec, D. L. Cooper, *Faraday Discuss.* **2007**, *135*, 31-42.

[34] R. Ponec, *Comput. Theor. Chem.* **2015**, *1053*, 195-213.

[35] D. L. Cooper, R. Ponec, *PCCP* **2008**, *10*, 1319-1329.

[36] R. Ponec, D. L. Cooper, A. Savin, *Chem. Eur. J.* **2008**, *14*, 3338-3345.

[37] R. Ponec, D. L. Cooper, *Struct. Chem.* **2017**, *28*, 1033-1043.

[38] R. F. W. Bader, *Atoms in Molecules. A Quantum Theory*, Oxford University Press, Oxford, **1990**.

[39] T. A. Keith, *AIMAll (Version 17.11.14)*, TK Gristmill Software, Overland Park KS, USA, see aim.tkgristmill.com.

[40] G. Schaftenaar, J. H. Noordik, *J. Comput. Aided Mol. Des.* **2000**, *14*, 123-134.

[41] A. M. K. Müller, *Phys. Lett. A* **1984**, *105*, 446-452.

[42] R. Ponec, D. L. Cooper, *THEOCHEM* **2005**, *727*, 133-138.

[43] X. Fradera, M. A. Austen, R. F. W. Bader, *J. Phys. Chem. A* **1999**, *103*, 304-314.

[44] I. Mayer, *Chem. Phys. Lett.* **2012**, *544*, 83-86.

[45] D. L. Cooper, R. Ponec, M. Kohout, *Mol. Phys.* **2016**, *114*, 1270-1284.

GRAPHICAL ABSTRACT

AUTHORS: Fabio E. Penotti, David L. Cooper, Peter B. Karadakov, and Robert Ponec

TITLE: Nature of the chemical bonding in D_{3h} [MH$_3$M]$^+$ cations (M = Be, Mg)

TEXT: The bonding situation in [MH$_3$M]$^+$ cations (M = Be, Mg), which feature very short metal-metal distances, is shown to be well described by three equivalent highly polar three-center two-electron M−H−M bonding units, with the absence of direct metal-metal bonds.

GRAPHICAL ABSTRACT FIGURE:
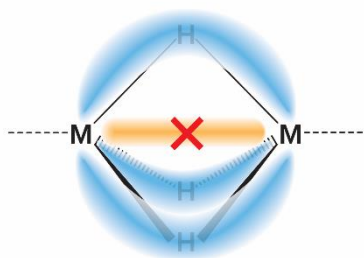
Supporting Information

Nature of the chemical bonding in D_{3h} [MH₃M]⁺ cations (M = Be, Mg)

Fabio E. Penotti[1], David L. Cooper[2], Peter B. Karadakov[3] and Robert Ponec[4]

[1]Consiglio Nazionale delle Ricerche, Istituto di Scienze e Tecnologie Chimiche "Giulio Natta", Via Golgi 19, I-20133 Milano MI, Italy

[2]Department of Chemistry, University of Liverpool, Liverpool L69 7ZD, United Kingdom

[3]Department of Chemistry, University of York, Heslington, York YO10 5DD, United Kingdom

[4]Institute of Chemical Process Fundamentals, Czech Academy of Sciences Prague 6, Suchdol 2, 165 02 Czech Republic

Table of Contents

Table of Contents (continued)

S1. Energies for D_{3h} [MH$_3$M]$^+$ and [NgMH$_3$MNg]$^+$ cations (M = Be, Mg)

Table S1.   Total energies (cc-pVQZ basis) for [MH$_3$M]$^+$ and [NgMH$_3$MNg]$^+$ cations, calculated at
the all-electron CCSD(T)/cc-pVQZ D_{3h} geometries.

	M = Be			M = Mg	
Method	'bare'	Ng = He	Ng = Ne	'bare'	Ng = He
RHF	-30.692417	-36.434555	-287.801165	-400.699443	-406.428468
SCGVB(6)	-30.728105	-36.470178	-287.836597	-400.736924	-406.465702
CASSCF(6,6)	-30.729260	-36.471315	-287.837759	-400.737151	-406.465922
CASSCF(6,11)	-30.774290	-36.515549	-287.880005	-400.770221	-406.498915
CCSD(T)	-30.884913	-36.717176	-288.672113	-400.901366	-406.715659
B3LYP	-30.967936	-36.824799	-288.951241	-401.711673	-407.549931

S2. Additional results for D_{3h} [BeH$_3$Be]$^+$ and [NgBeH$_3$BeNg]$^+$ cations
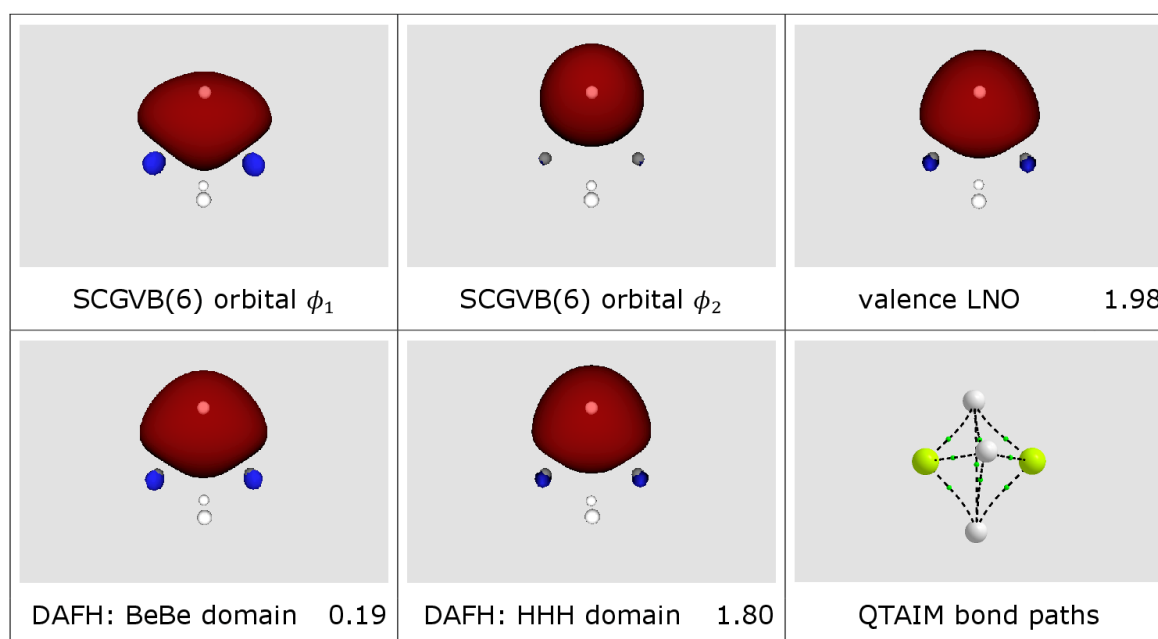
Figure S1.   Symmetry-unique key functions (and occupation numbers where appropriate) from
analysis of the SCGVB(6) description of the D_{3h} [BeH$_3$Be]$^+$ cation. Also shown are
QTAIM bond paths. (See also Figure 2.)

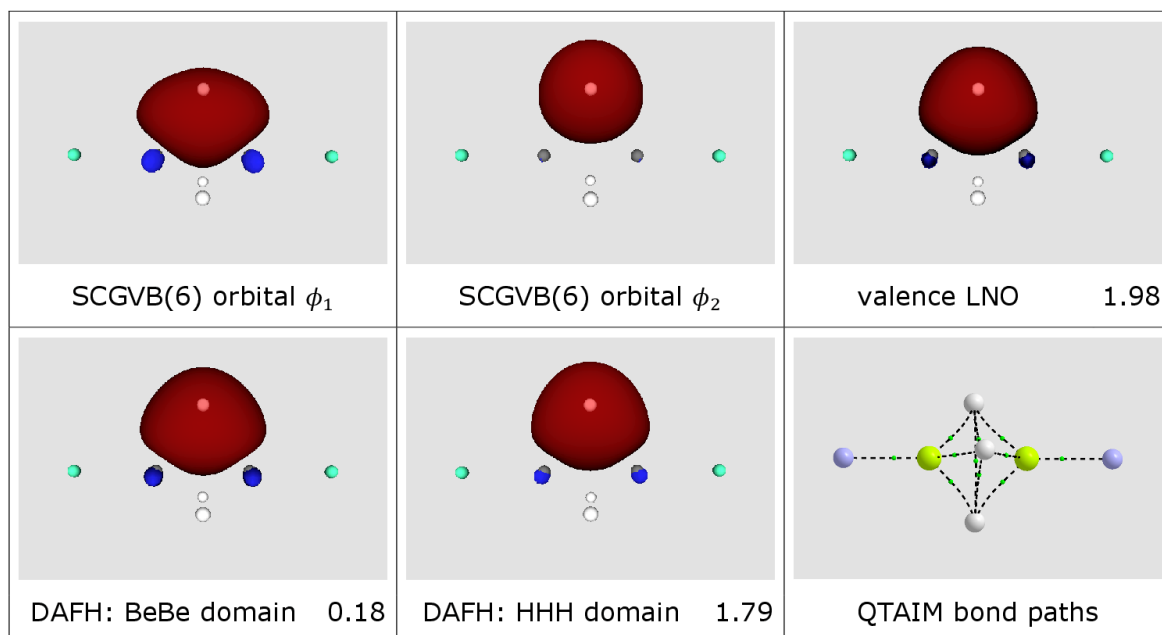| SCGVB(6) orbital ϕ_1 | SCGVB(6) orbital ϕ_2 | valence LNO   1.98 |
| DAFH: BeBe domain   0.19 | DAFH: HHH domain   1.80 | QTAIM bond paths |

Figure S2. Symmetry-unique key functions (and occupation numbers where appropriate) from analysis of the SCGVB(6) description of the D_{3h} [HeBeH$_3$BeHe]$^+$ cation. Also shown are QTAIM bond paths.

| SCGVB(6) orbital ϕ_1 | SCGVB(6) orbital ϕ_2 | valence LNO 1.98 |
| DAFH: BeBe domain 0.18 | DAFH: HHH domain 1.79 | QTAIM bond paths |

Figure S3. Symmetry-unique key functions (and occupation numbers where appropriate) from analysis of the SCGVB(6) description of the D_{3h} [NeBeH$_3$BeNe]$^+$ cation.

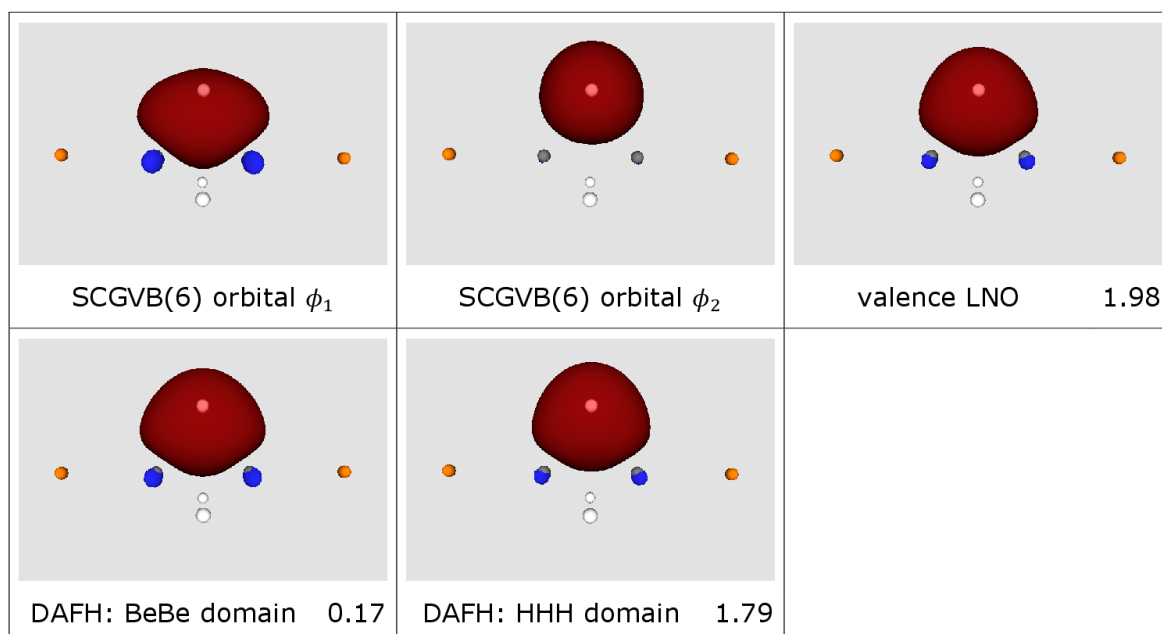| SCGVB(6) orbital ϕ_1 | SCGVB(6) orbital ϕ_2 | valence LNO 1.98 |
| DAFH: BeBe domain 0.17 | DAFH: HHH domain 1.79 | |

Figure S4. Symmetry-unique dominant valence LNOs (and occupation numbers) for the D_{3h} [BeH$_3$Be]$^+$ cation obtained with different methods.
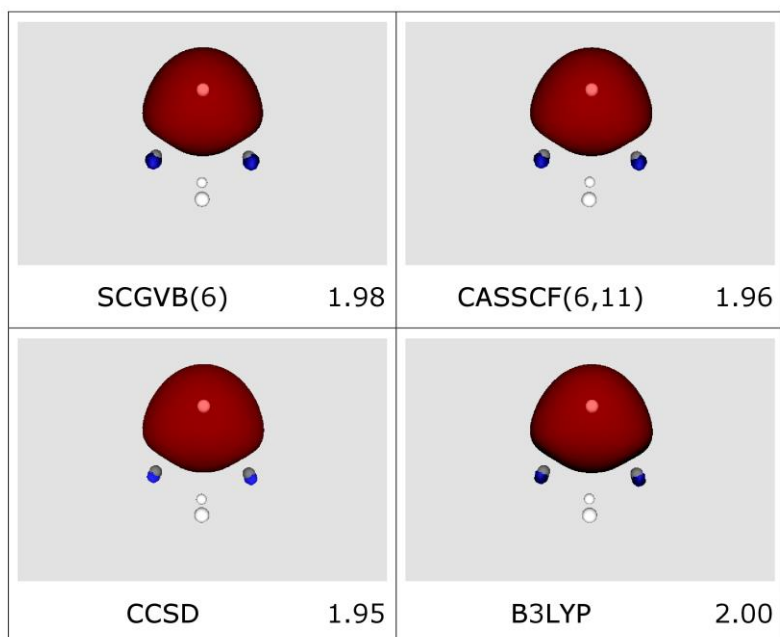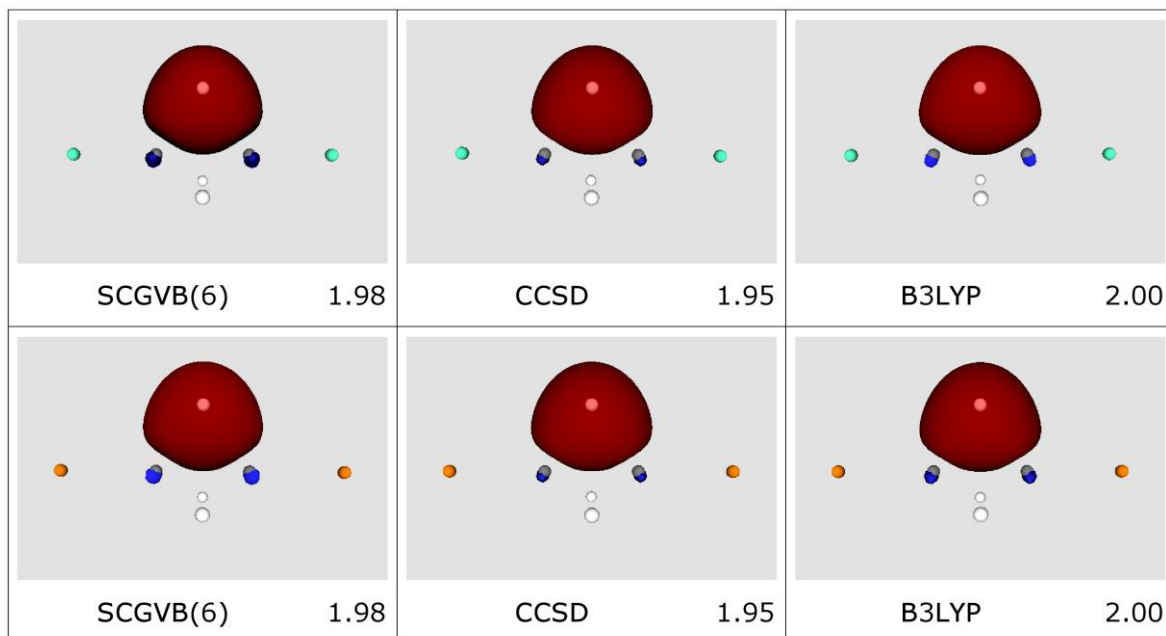

Figure S5. Symmetry-unique dominant valence LNOs (and occupation numbers) for D_{3h} [NgBeH$_3$BeNg]$^+$ cations obtained with different methods: top row, Ng = He; bottom row, Ng = Ne.

S3. Additional results for D_{3h} [MgH₃Mg]⁺ and [HeMgH₃MgHe]⁺ cations

Figure S6.   Symmetry-unique key functions (and occupation numbers where appropriate) from analysis of the SCGVB(6) description of the D_{3h} [MgH₃Mg]⁺ cation. Also shown are QTAIM bond paths. (See also Figure 3.)

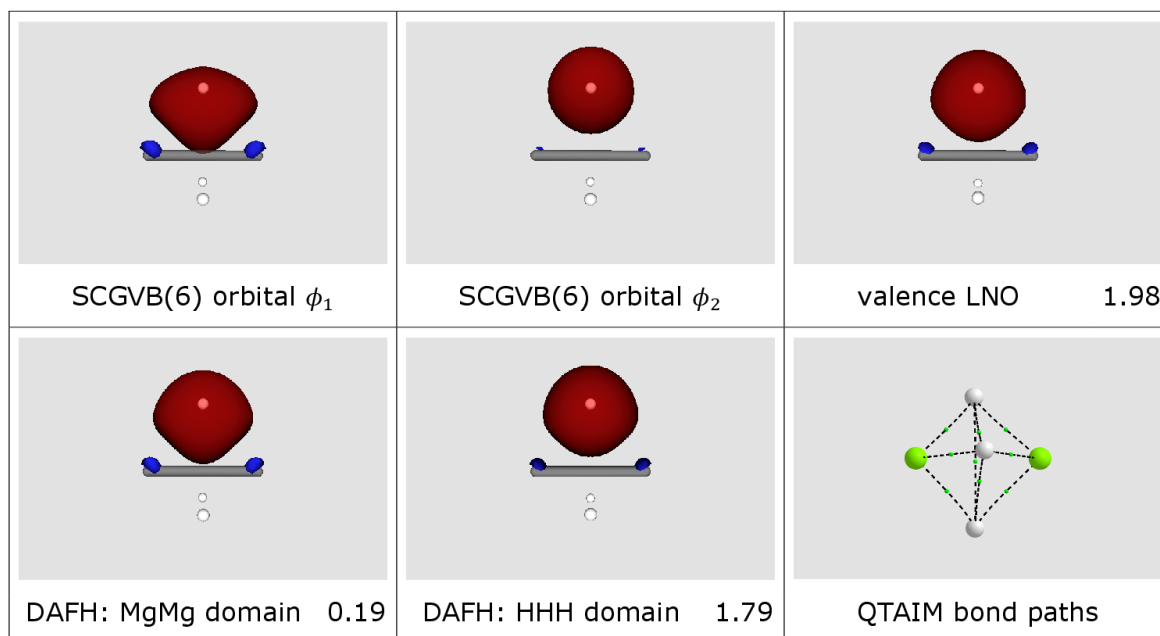| SCGVB(6) orbital ϕ_1 | SCGVB(6) orbital ϕ_2 | valence LNO   1.98 |
| DAFH: MgMg domain   0.19 | DAFH: HHH domain   1.79 | QTAIM bond paths |

Figure S7.   Symmetry-unique key functions (and occupation numbers where appropriate) from analysis of the SCGVB(6) description of the D_{3h} [HeMgH₃MgHe]⁺ cation. Also shown are QTAIM bond paths.

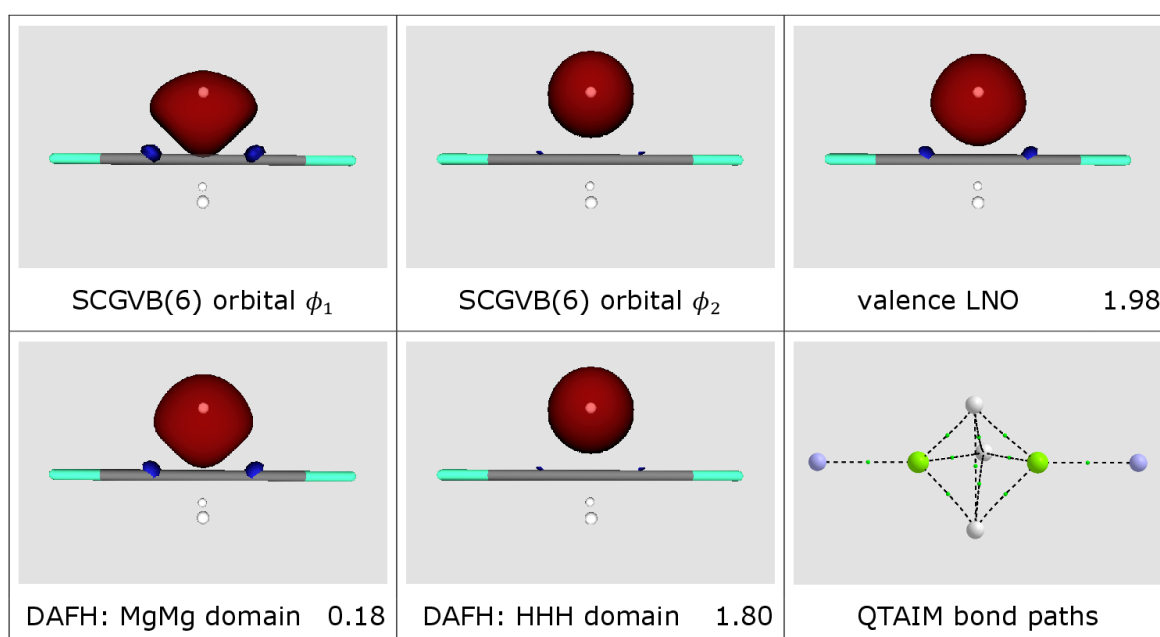| SCGVB(6) orbital ϕ_1 | SCGVB(6) orbital ϕ_2 | valence LNO   1.98 |
| DAFH: MgMg domain   0.18 | DAFH: HHH domain   1.80 | QTAIM bond paths |

Figure S8. Symmetry-unique dominant valence LNOs (and occupation numbers) for the D_{3h} $[MgH_3Mg]^+$ cation obtained with different methods.

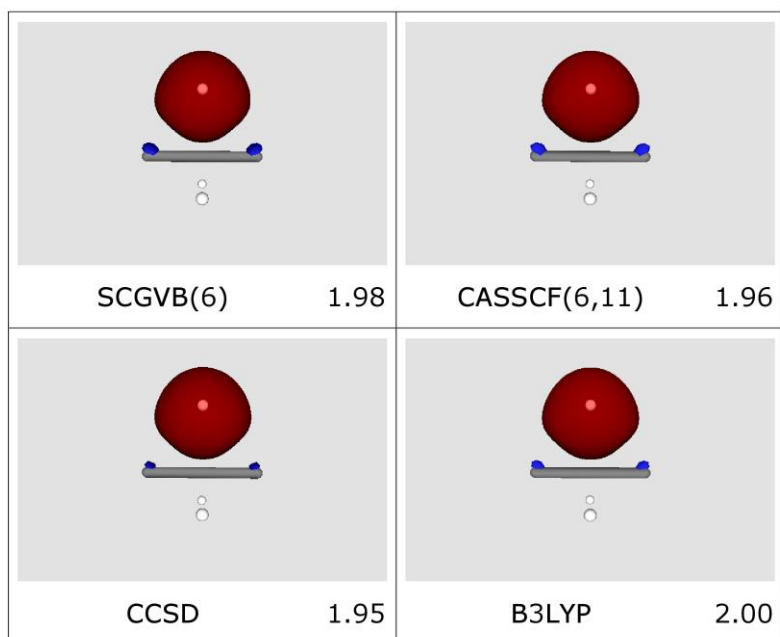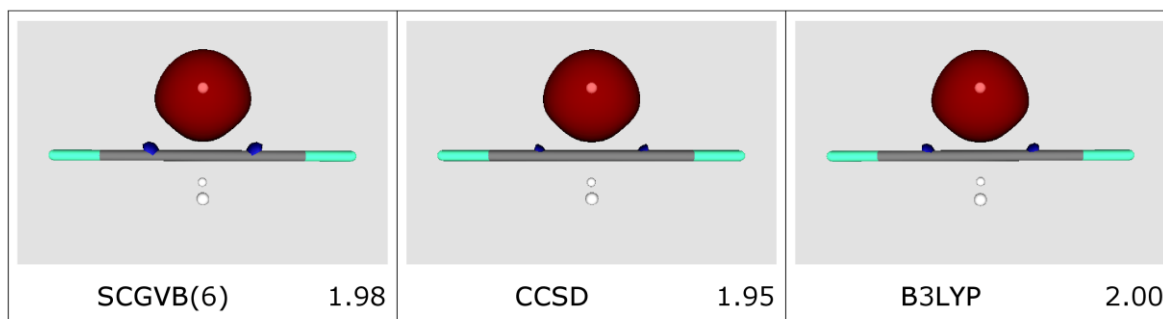|	
SCGVB(6) 1.98	CASSCF(6,11) 1.96
CCSD 1.95	B3LYP 2.00

Figure S9. Symmetry-unique dominant valence LNOs (and occupation numbers) for the D_{3h} $[HeMgH_3MgHe]^+$ cation obtained with different methods.

SCGVB(6) 1.98	CCSD 1.95	B3LYP 2.00

S4. Results for the 'mixed' C_{3v} [BeH$_3$Mg]$^+$ and [HeBeH$_3$MgHe]$^+$ cations

Table S2. Distances (Å) and angles (degrees) for C_{3v} [NgBeH$_3$MgNg]$^+$ cations optimized at the all-electron CCSD(T)/cc-pVQZ level of theory.

Ng	r_{BeMg}	r_{BeH}	r_{MgH}	r_{NgBe}	r_{NgMg}	θ_{BeHMg}	θ_{MgBeH}
	2.003	1.426	1.862			73.71	63.15
He[a]	2.005	1.429	1.853	1.494	1.960	74.03	62.70

[a] Although this C_{3v} geometry does not correspond to a local minimum, the energy lowering to a C_s structure with a non-collinear HeBeMgHe arrangement is very small indeed (40.3 microhartree).

Table S3. Total energies (cc-pVQZ basis) for C_{3v} [BeH$_3$Mg]$^+$ and [HeBeH$_3$MgHe]$^+$ cations, calculated at the all-electron CCSD(T)/cc-pVQZ C_{3v} geometries.

Method	'bare'	Ng = He
RHF	-215.706253	-221.438923
SCGVB(6)[a]	-215.742309	-221.474799
CASSCF(6,6)	-215.742893	-221.475385
CASSCF(6,11)	-215.786453	-221.518662
CCSD(T)	-215.904013	-221.724970
B3LYP	-216.349310	-222.194517

[a] These SCGVB(6) wavefunctions incorporate 98.4% of the non-dynamical correlation energy that is retrieved with the corresponding CASSCF(6,6) calculations, with the energy differences between the two descriptions being very small (*ca*. 1.5 kJ/mol);. Increasing the number of active orbitals to 11, as in CASSCF(6,11), retrieved further energy lowerings of *ca*. 115 kJ/mol.

Figure S10. Symmetry-unique key functions (and occupation numbers where appropriate) from analysis of the SCGVB(6) description of the C_{3v} [BeH$_3$Mg]$^+$ cation. Also shown are QTAIM bond paths. The BeMg axis runs from left to right.

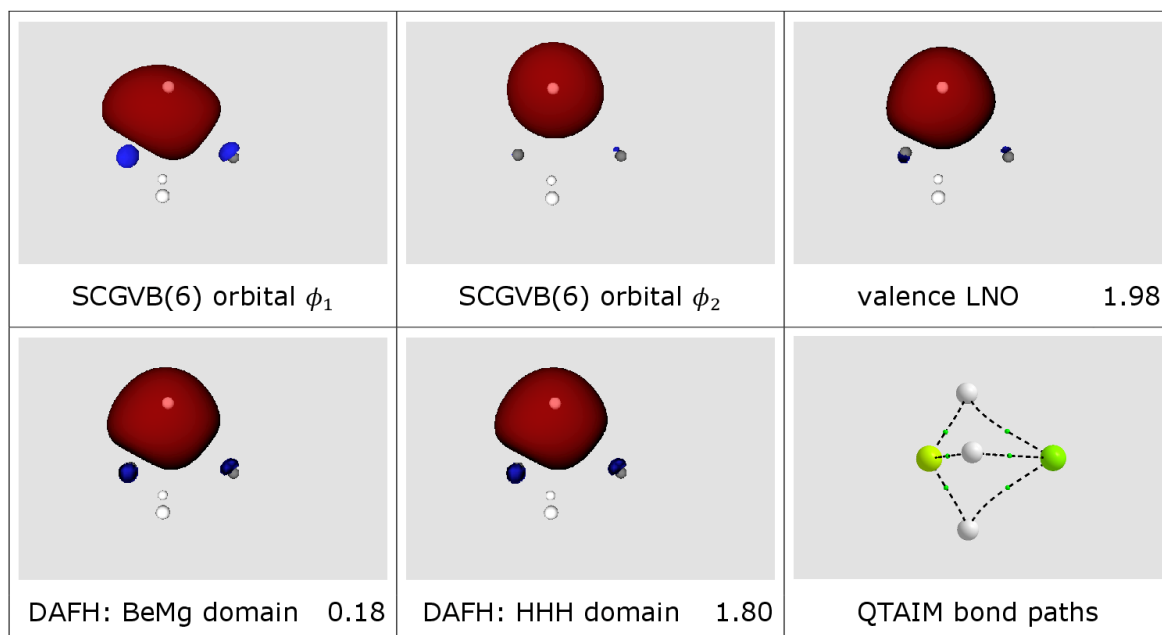| SCGVB(6) orbital ϕ_1 | SCGVB(6) orbital ϕ_2 | valence LNO   1.98 |
| DAFH: BeMg domain   0.18 | DAFH: HHH domain   1.80 | QTAIM bond paths |

Figure S11. Symmetry-unique key functions (and occupation numbers where appropriate) from analysis of the SCGVB(6) description of the C_{3v} [HeBeH$_3$MgHe]$^+$ cation. Also shown are QTAIM bond paths. The BeMg axis runs from left to right.

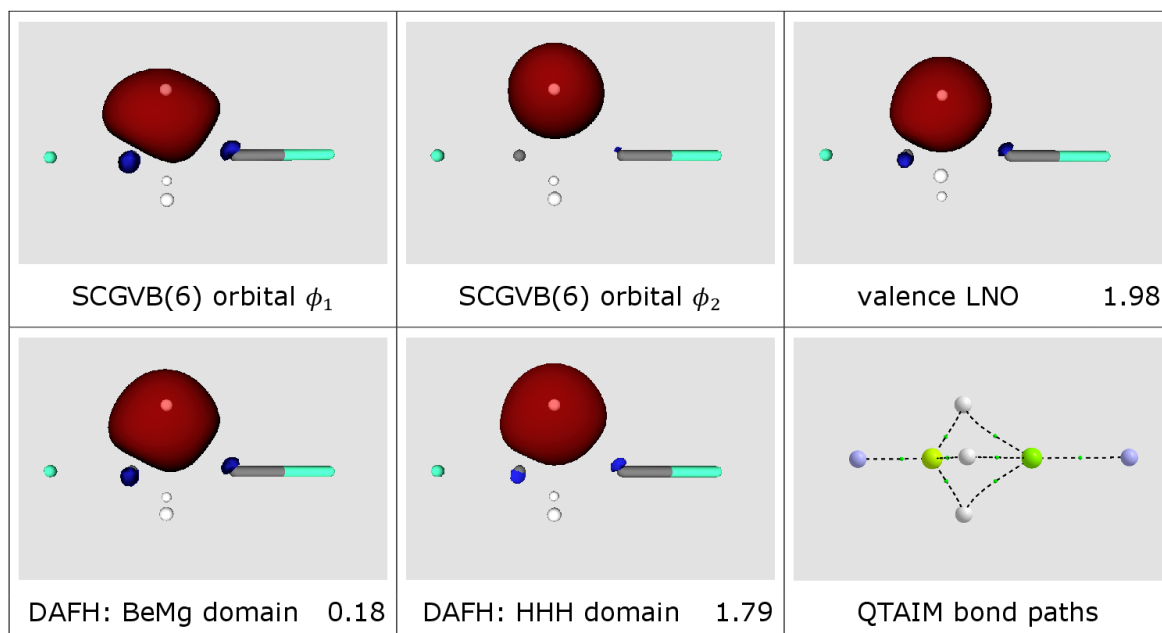| SCGVB(6) orbital ϕ_1 | SCGVB(6) orbital ϕ_2 | valence LNO   1.98 |
| DAFH: BeMg domain   0.18 | DAFH: HHH domain   1.79 | QTAIM bond paths |

Figure S12. Symmetry-unique dominant valence LNOs (and occupation numbers) for the C_{3v} [BeH$_3$Mg]$^+$ cation obtained with different methods. The BeMg axis runs from left to right.
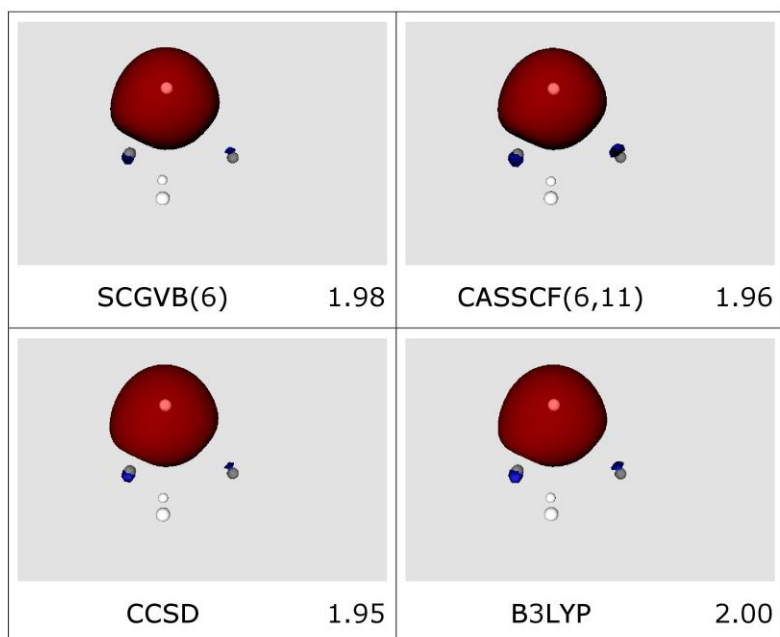

Figure S13. Symmetry-unique dominant valence LNOs (and occupation numbers) for the C_{3v} [HeBeH$_3$MgHe]$^+$ cation obtained with different methods. The BeMg axis runs from left to right.